Optical Properties of Eu^{2+} in α-SiAlON

Rong-Jun Xie,* Naoto Hirosaki, Mamoru Mitomo, Yoshinobu Yamamoto, and Takayuki Suehiro

Advanced Materials Laboratory, National Institute for Materials Science, Namiki 1-1, Tsukuba, Ibaraki 305-0044, Japan

Ken Sakuma

Optical Communication Technology Department, Fujikura Ltd., Mutsuzaki 1440, Sakura, Chiba 285-8550, Japan

Received: April 19, 2004; In Final Form: May 31, 2004

New interesting α-SiAlON:Eu-based yellow oxynitride phosphors with the formula $(Ca_xEu_y)Si_{12-2x-3y}Al_{2x+3y}O_yN_{16-y}$ ($x = 0.2-2.2$, $y = 0-0.25$) have been prepared, and the effects of the activator concentration and the overall composition of the host lattice on optical properties have been investigated. It has been demonstrated that the Eu^{2+}-doped α-SiAlON phosphors absorb strongly in the UV−visible part of the electromagnetic spectrum and exhibit an intense emission band with peaks at 583−605 nm. We have shown that the optical properties depend greatly on the Eu^{2+} concentration and the overall composition of the host lattice. The results indicate a concentration quenching effect at $y \geq 0.075$ and a systematic red-shift in emission wavelength as the Ca^{2+} or the Eu^{2+} concentration increases.

Introduction

Rare-earth (RE)-activated oxynitride or nitride luminescent materials have attracted much attention in recent years due to their nontoxicity, interesting luminescence properties, and potential applications as phosphors and pigments.[1−7] Examples include Y−Si−O−N:Ce^{3+},[1] $LaSi_3N_5$:Eu^{3+},[2] $M_2Si_5N_8$:Eu^{2+} (M = Ca, Sr, or Ba),[3] $Ca_{1-x}La_xTaO_{2-x}N_{1+x}$,[4] and Eu^{2+}-, Ce^{3+}-, or Tb^{3+}-doped α-SiAlONs.[5−7] Among these (oxy)nitride luminescence materials, Eu^{2+}-doped α-SiAlON represents a new class of yellow phosphors with high efficiency; it has strong absorption in the UV−visible spectral region and exhibits a broad emission band peaking at 550−590 nm.[5,6] Therefore, this novel yellow α-SiAlON:Eu phosphor is expected to have applications in white LEDs when a GaN-based blue chip is coupled.[8] In addition, due to the unique crystal structure of α-SiAlON, the α-SiAlON host lattice has advantages of (i) better flexibility of material design without changing the crystal structure, (ii) composition-tunable luminescence properties, and (iii) higher thermal stability in luminescence efficiency and emission color compared to its sulfide, oxide, or halide counterparts.

α-SiAlON is isostructural to α-Si_3N_4.[9] The α-SiAlON unit cell content, consisting of four "Si_3N_4" units, can be given in a general formula $M^{val+}_{m/val}Si_{12-m-n}Al_{m+n}O_nN_{16-n}$.[9−11] In the α-SiAlON structure, $m + n$ Si−N bonds are replaced by m Al−N bonds and n Al−O bonds; the charge discrepancy caused by the substitution is compensated by the introduction of the M cations including Li, Mg, Ca, Y, and lanthanides except La, Ce, and Eu. The M cations occupy the interstitial sites in the α-SiAlON lattice and are coordinated by seven N, O anions at three different M−(N, O) distances.[12] It is generally accepted that the Eu^{2+} ion alone cannot stabilize the α-SiAlON structure due to its large ionic size, but it does if codoped with calcium.[5,6] Our previous study indicates that Ca-α-SiAlON entirely prepared from nitrides (i.e., Si_3N_4, AlN, and Ca_3N_2) has a wider single-phase forming area (i.e., higher solubility) than that prepared from Si_3N_4, AlN, and CaO.[13] Therefore, in this work Ca-α-SiAlON entirely prepared from nitrides (with a formula of $Ca_xSi_{12-m}Al_mN_{16}$, $x = m/2$) is selected as the host lattice with aims to (i) realize a high solubility limit of Eu^{2+} ions and (ii) investigate the effect of a broader composition of the host lattice on the luminescence properties.

The luminescence of Eu^{2+}, originating from the $4f^7 \leftrightarrow 4f^65d$ transition, strongly relies on the environment (i.e., crystal field) acting on the Eu^{2+} ions[14] and also the concentration of Eu^{2+} itself. This allows one to tailor the luminescence properties of α-SiAlON:Eu phosphors (efficiency, emission color, quenching effect, etc.) by careful material designs. In the preliminary work on Eu^{2+}-doped α-SiAlON, the main focus has been on the preparation and the photoluminescence spectra; little attention has been paid on the composition effects (i.e., the activator concentration and the host lattice composition). The present investigation provides a comprehensive study of the Eu^{2+}-doped α-SiAlON phosphors to reveal the structural evolution, the compositional dependence of optical properties, and the concentration quenching effect.

Experimental Section

Eu^{2+}-doped Ca-α-SiAlON phosphors with the compositions of $(Ca_xEu_y)Si_{12-2x-3y}Al_{2x+3y}O_yN_{16-y}$ ($x = 0.2-2.2$, $y = 0-0.25$), were prepared from α-Si_3N_4 (SN-E10, Ube Industries, Japan), AlN (Tokuyama Corp., type F, Japan), Ca_3N_2 (Kojundo Chemical Laboratory Co. Ltd., Japan), and Eu_2O_3 (Shin-Etsu Chemical Co. Ltd, Japan). Due to the air and moisture sensitivity of Ca_3N_2, the powder mixture was made under a continuously purified nitrogen atmosphere in a glovebox (MBRAUN Unilab, MBRAUN GmbH, Germany). The concentration of oxygen and

* Corresponding author. Tel: +81-29-860-4312. Fax: +81-29-851-3613. E-mail: Xie.Rong-Jun@nims.go.jp.

10.1021/jp048295g CCC: $27.50
Published on Web 07/20/2004

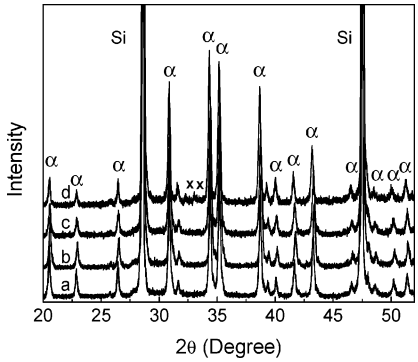

Figure 1. XRD spectra of samples doped with different amounts of europium ($x = 0.625$), showing the solubility limit of europium at $y = 0.20$: (a) $y = 0$; (b) $y = 0.075$; (c) $y = 0.10$; (d) $y = 0.20$.

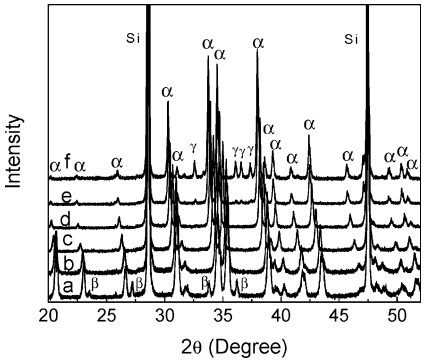

Figure 2. XRD spectra showing the progressive peak shift and phase change in samples having various overall compositions ($y = 0.075$): (a) $x = 0.2$; (b) $x = 0.3$; (c) $x = 1.05$; (d) $x = 1.8$; (e) $x = 1.9$; (f) $x = 2.0$; α = α-SiAlON; β = β-SiAlON; γ = $CaAlSiN_3$.

moisture is <1 ppm. The powder was then synthesized by gas-pressure sintering (GPS) at 1800 °C for 2 h under 10 atm of N_2. The Eu^{3+} ion in the starting powder Eu_2O_3 is reduced to Eu^{2+} under the nitrogen atmosphere during sintering, which is confirmed by the absorption and emission spectra given later.

The phase products of synthesized powders were identified by X-ray powder diffraction (XRD, Philips PW1700), operating at 40 kV and 40 mA and using Cu Kα radiation ($\lambda = 1.5406$ Å). A step size of 0.005° 2θ was used with a scan speed of 0.5° per minute. For determination of the lattice parameters of α-SiAlON, silicon was used as the internal standard. The powder morphology was investigated by scanning electron microscopy (SEM), JEOL-840A. The particle size distribution was measured with a laser diffraction system, CILAS1064.

The luminescence spectra were measured at room temperature using a fluorescent spectrophotometer (F-4500, Hitachi Ltd., Japan) with a 150 W Ushio xenon short arc lamp. The emission spectrum was corrected for the spectral response of a monochromator and Hamamatsu R928P photomultiplier tube by a light diffuser and tungsten lamp (Noma, 10 V, 4 A). The excitation spectrum was also corrected for the spectral distribution of the xenon lamp intensity by measuring rhodamine-B as reference. The diffusive reflection spectrum was recorded on a UV−vis spectrophotometer with an integrating sphere (JASCO, Ubest V-560). The reflection spectrum of Spectralon diffusive white standards is used for calibration (the reflectivity is nearly 100% in the range of 200−900 nm).

Results and Discussion

Structural Characterization. Figure 1 shows XRD patterns of samples doped with different europium concentrations ($x = 0.625$). Note that a single α-SiAlON phase is formed in compositions with $y < 0.20$. Besides the major α-SiAlON phase, an unknown phase (marked by "x") is traceable in the composition of $y = 0.20$, suggesting that the solubility limit of Eu^{2+} in α-SiAlON is less than 0.20. The variation in relative peak intensities and positions compared to that of the nondoped Ca-α-SiAlON indicates lattice distortion and incorporation of Eu^{2+} in the α-SiAlON lattice. Figure 2 gives the XRD spectra of samples with various overall compositions ($y = 0.075$). One can define a single α-SiAlON phase region at $0.3 \leq x \leq 1.8$ (i.e., $0.75 \leq m \leq 3.75$, $m = 2x + 2y$). The α-SiAlON forming region in the present study is somewhat wider than that reported in our previous work ($0.5 \leq x \leq 1.7$), which is partly due to the different sample preparation methods. The β-phase is observed to coexist with α-SiAlON when x is below 0.3, whereas the $CaSiAlN_3$ phase (JCPDS Cards No. 39-0747) tends to form when x is over 1.8. It is clearly seen that the diffraction peak progressively shifts to low diffraction angle with increasing

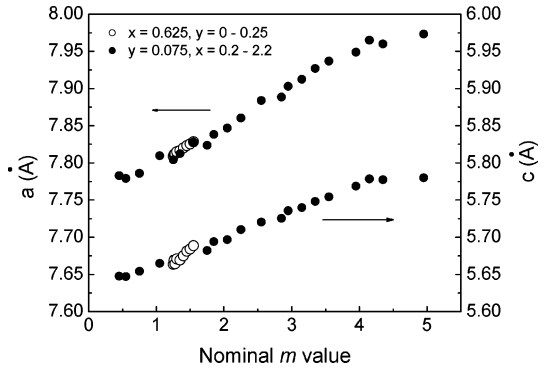

Figure 3. Lattice parameters of samples with different compositions.

Ca^{2+} concentration (i.e., the m value), indicating continued expansion of the crystal lattice as shown below.

Cell parameters of compositions with varying x and y as a function of the nominal m value are shown in Figure 3. Note that a linear relationship between the lattice parameter and the m value is observed in the single α-SiAlON phase region. Beyond the single α-SiAlON phase region, the lattice parameters remain constant. The increment of cell dimension is attributable to the increased m and n values, since the average Si−N bond length of 1.74 Å is shorter than that of Al−N (1.87 Å) and Al−O (1.75 Å).[9] Moreover, with the same m value, the lattice parameters of the compositions with varying y value (while the Ca^{2+} concentration is fixed at $x = 0.625$) are nearly equal to those of the compositions with varying x value (while the Eu^{2+} concentration is fixed at $y = 0.075$). It indicates that the ionic size of Eu^{2+} or Ca^{2+} ions has little influence on the unit cell dimension of α-SiAlON. The lattice expansion caused by partial substitution for Si−N bonds must change the crystal field surrounding the Eu^{2+} ions, which would finally affect luminescence properties of Eu^{2+}-doped α-SiAlONs.

Figure 4 shows an electron microscope image of a typical α-SiAlON:Eu phosphor ($x = 0.625$, $y = 0.075$). The mostly equiaxed and some hexagonally shaped crystals of 0.5−1.8 μm size grow together and form larger aggregates, which are partially broken up again in a mortar. The powder is uniform and exhibits a narrow particle size distribution, as shown in Figure 5.

Diffuse Reflectance Spectra. UV−visible diffuse reflectance spectra of selected samples doped with different amounts of Eu^{2+} ions are depicted in Figure 6. As seen, nondoped α-SiAlON is white in color and shows an absorption edge only in the UV part of the electromagnetic spectrum (~297 nm). Eu^{2+}-doped α-SiAlONs, however, show strong absorption in

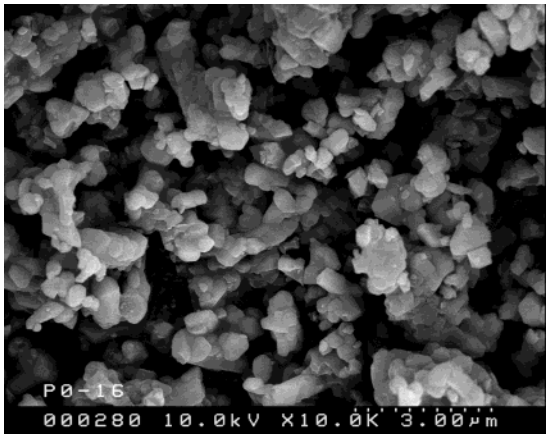

Figure 4. SEM image of an α-SiAlON powder phosphor ($x = 0.625$, $y = 0.075$).

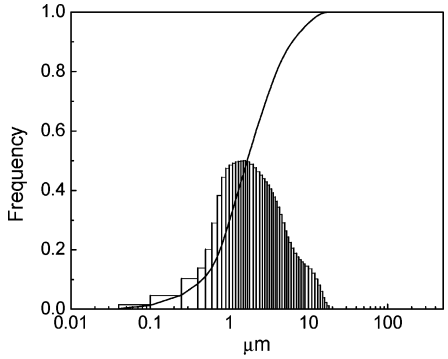

Figure 5. Particle size distribution of an α-SiAlON powder phosphor ($x = 0.625$, $y = 0.075$).

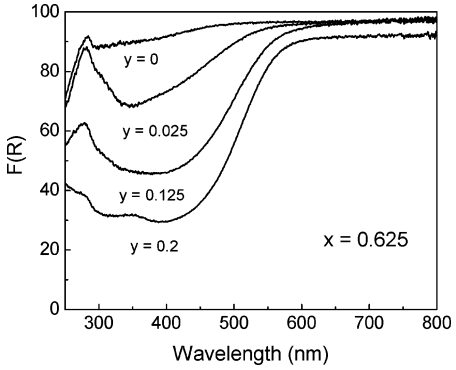

Figure 6. UV−vis diffuse reflectance spectra of α-SiAlON:Eu phosphors doped with different amounts of europium.

the UV to visible spectral region, which can be assigned to Eu^{2+}. Meanwhile, there is a shift in the onset of absorption to lower energy (red shift) on increase of Eu^{2+} concentration. This red shift is consistent with that observed in the emission band as the Eu^{2+} concentration increases, and the latter is ascribed to the large Stokes shift and the splitting of 5d orbitals of Eu^{2+}-(shown later). The color of Eu^{2+}-doped α-SiAlONs, therefore, varies from light yellow to orange with increasing Eu^{2+} concentration.

The red shift in the absorption edge can also be explained by the changes in the optical band gap of α-SiAlON as its composition varies with Eu^{2+} doping. Estimates of the optical band gap (E_g) can be obtained using the following equation for a semiconductor:[15]

$$\alpha h\nu = A(h\nu - E_g)^{q/2} \quad (1)$$

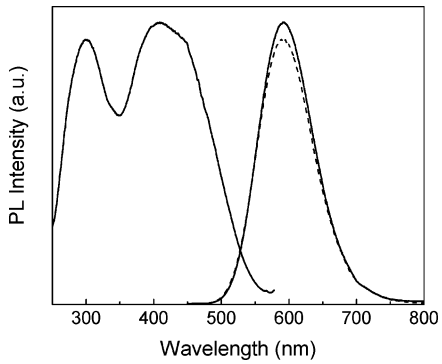

Figure 7. Typical excitation and emission spectra for α-SiAlON:Eu phosphors. This sample contains a calcium content of $x = 0.10$ and a europium concentration of $y = 0.075$ ($\lambda_{em} = 590$ nm; $\lambda_{exc} = 410$ nm for the solid line or $\lambda_{exc} = 305$ nm for the dashed line).

where α, ν, A, and E_g are absorption coefficient, light frequency, proportionality constant, and band gap, respectively. The variable q describes the nature of the transition in a semiconductor: 1 or 3 for a direct allowed transition and 4 or 6 for an indirect transition. The absorption coefficient, α, is proportional to $F(R)$ with the Kubelka−Munk function, $F(R)^2/[2(1 - F(R))]$. The values of q and E_g were determined by the following steps:[16] first, plot $\ln(\alpha h\nu)$ vs $\ln(h\nu - E_g)$ using an approximate value of E_g, and then determine the value of q with the slope of the straight line near the band edge; second, plot $(\alpha h\nu)^{2/q}$ vs $h\nu$, and then evaluate the band gap E_g by extrapolating the straight line to $(\alpha h\nu)^{2/q} = 0$. When this method is used, the q value is determined as 4, indicating the indirectly allowed optical transition of Eu^{2+}-doped Ca-α-SiAlON. The band gap E_g is about 4.45 eV for the nondoped α-SiAlON, which is smaller than the reported optical band gap of α-Si_3N_4 (5.0−5.2 eV). This discrepancy may be due to the partial replacement of Si−N by Al−N and Al−O in α-SiAlON. It has been reported that the optical band gap of β-SiAlON ($Si_{8-z}Al_zO_zN_{6-z}$) decreases with increasing z value.[17] The optical band gap is significantly reduced as the Eu^{2+} ions are introduced; it decreases to 2.50 eV for the sample with $y = 0.005$ and to 2.19 eV for the sample with $y = 0.20$.

Photoluminescence Properties. Figure 7 shows typical excitation and emission spectra of α-SiAlON:Eu phosphors. The sample shown here has the composition of $x = 0.625$ and $y = 0.10$. The excitation spectrum is broad and structureless. It covers the spectral region from the UV to the visible part, which is consistent with the reflection spectrum. Two broad bands are observed in the excitation spectrum with maxima at 305 and 412 nm. The first band is assigned to absorption of the host lattice (α-SiAlON), and the second one corresponds to $4f^7 \rightarrow 4f^65d$ transition of Eu^{2+}. The emission spectrum shows a single intense broad emission band at 592 nm. This emission band is attributable to the allowed $4f^65d \rightarrow 4f^7$ transition of Eu^{2+}. The characteristic luminescence of Eu^{3+} is not observed, which exhibits sharp lines between 580 and 650 nm. This suggests that the europium ion in α-SiAlON is in the divalent state. The observed unusual long-wavelength excitation and emission bands result from the nitrogen-rich surrounding of Eu^{2+} ions in α-SiAlON, as mentioned previously.[5,6] Both the higher formal charge of N^{3-} compared with O^{2-} and the lower electronegativity of nitrogen (3.04) compared with oxygen (3.44) (nephelauxetic effect) would lead to larger ligand-field splitting of the 5d levels and the center of gravity of the 5d states at lower energy. It is also suggested that the preferential orientation of a d-orbital or low-lying state of the conduction band would account for the long emission wavelength.[3] The Stokes shift of

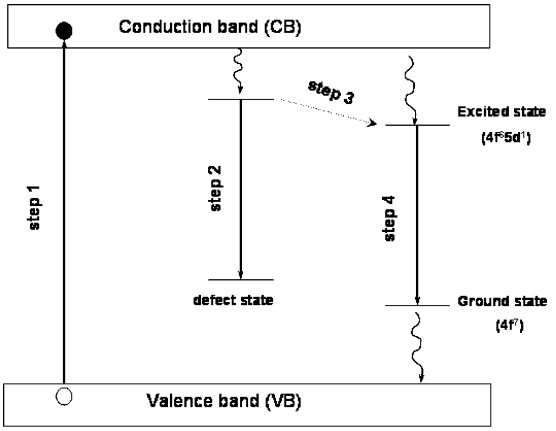

Figure 8. Schematic band-gap model for the luminescence of Eu^{2+} in α-SiAlON.

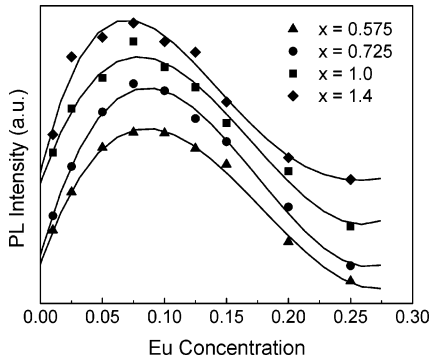

Figure 9. Graph of emission intensity vs the europium concentration indicating the concentration quenching at $y = 0.075$.

the Eu^{2+}-doped α-SiAlON, roughly calculated from the spectral data, varies in the range of 7000−8000 cm^{-1}, which is in good agreement with previous reports.[5,6] One explanation proposed by Krevel et al.[5] for this large Stokes shift is that the small size of the interstitial site in α-SiAlON promotes shrinkage of the Eu^{2+} ions in the excited state in comparison with the ground state, leading to a large relaxation and hence a large Stokes shift.

In doped semiconductors, two channels of excitations are responsible for the impurity luminescence. One is indirect excitation, that is, excitation into the conduction band of the host, followed by an energy transfer from the host to the impurity ions to cause the luminescence. The other is direct excitation of the impurity ions. As seen in the excitation spectrum, both the direct and indirect excitations are involved in Eu^{2+}-doped α-SiAlONs. Figure 8 schematically shows the band-gap model for the photoluminescence of Eu^{2+}-doped α-SiAlON. The excitation of electrons across the host lattice band gap from the valence to conduction band (step 1) is followed by radiative recombination with a deeply trapped hole at a defect state (step 2) or a nonradiative relaxation into the europium 5d level (step 3). Following step 3, a radiative transition from the excited state to the ground state of Eu^{2+} occurs (step 4), yielding the luminescence of Eu^{2+}. As shown in Figure 7, it is quite clear that the luminescence of Eu^{2+}-doped α-SiAlON obtained by direct excitation of the impurity ions ($\lambda_{exc} = 412$ nm) is more efficient than that obtained by the indirect excitation of the host ($\lambda_{exc} = 305$ nm).

Concentration Quenching and Composition Dependence of Photoluminescence. Figure 9 shows the emission intensity as a function of the Eu^{2+} concentration for different α-SiAlON host matrixes. For all α-SiAlONs, starting at low Eu^{2+} concentration, the emission intensity rises to a maximum at a Eu^{2+} concentration of $y = 0.075$ and falls again steadily to a minimum at $y = 0.25$. This decrease in emission intensity beyond a critical concentration can be explained by concentration quenching, which is mainly caused by the energy transfer between Eu^{2+} ions. The probability of energy transfer between two activator ions is inversely proportional to the nth power of R' ($n = 6$, 8, or 10) where R' is the distance between the activator ions.[18] When the concentration of Eu^{2+} increases, the distance between Eu^{2+} ions is small, and thus the probability of energy transfer increases. Figure 10 shows the dependence of the emission intensity on the composition of the α-SiAlON host matrix. The strongest luminescence is achieved at $x = 1.4$ as the concentration of Eu^{2+} is fixed at $y = 0.075$. The explanation for the compositional dependence is still unclear; the above result, however, implies that the luminescence properties of Eu^{2+}-doped α-SiAlONs can be tailored by controlling the overall composition of the host lattice.

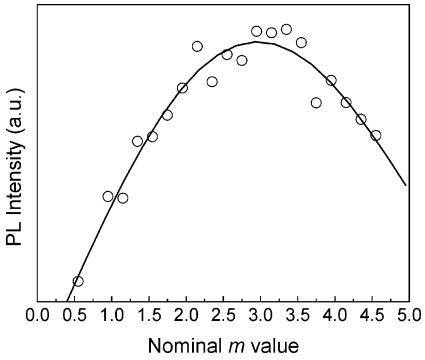

Figure 10. Graph of emission intensity vs the overall composition of the host lattice.

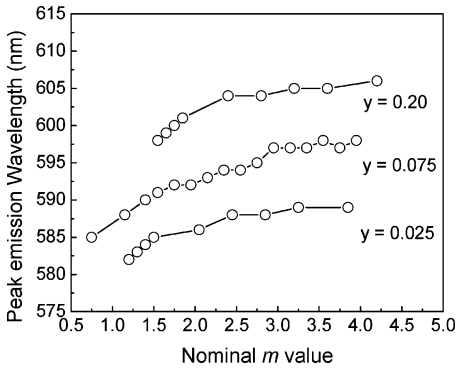

Figure 11. Graph of peak emission wavelength vs the overall composition of the host lattice.

Another interesting feature relating to the composition of the host α-SiAlON matrix and the Eu^{2+} concentration is the emission band shift. Figure 11 shows the maximum emission wavelength as a function of the nominal m value for different Eu^{2+} concentrations. Red shift of the emission band is observed when the m value or the Eu^{2+} concentration is increased. This shift may be due to some changes in the crystal field acting on the Eu^{2+} ions, which are caused by the lattice expansion and partial replacement of Si−N bonds. The increase in the m value implies larger numbers of shorter and stronger Si−N bonds replaced by longer and weaker Al−N bonds, thereby leading to less rigidity of the α-SiAlON lattice. As a result, the Stokes shift becomes larger with increasing the m value, which contributes to the red shift of the emission wavelength (the excitation wavelength remains unchanged). This is also the case when the Eu^{2+} concentration rises. In addition, the changes in crystal field may result in the splitting of 5d orbitals of Eu^{2+}.

As mentioned above, the probability of the energy transfer, from the Eu^{2+} ions at higher levels of 5d to those at the lower levels of 5d, increases with an increase of Eu^{2+} concentration. This makes it possible that higher Eu^{2+} concentration lowers the emission energy for transfer from the low 5d excited state to the 4f ground state and hence shifts the emission to long wavelength.

Conclusions

Novel yellow α-SiAlON:Eu phosphors have been synthesized by gas-pressure sintering at 1800 °C for 2 h under 10 atm of N_2. Their optical properties have been evaluated by the UV−visible diffuse reflectance spectrum and photoluminescence spectra at room temperature. The effects of the activator concentration and the overall composition of host lattice on the optical properties of Eu^{2+} in α-SiAlON have been discussed. The absorption edge shifts to longer wavelength with increasing Eu^{2+} concentration, resulting in changes in color from light yellow to orange. Luminescence concentration quenching occurs at a Eu^{2+} concentration of 0.075 and higher. This is explained by the energy transfer between Eu^{2+} ions. A systematic red shift of the emission band is observed as the Eu^{2+} concentration or the Ca^{2+} content increases, which is due to less rigidity of lattice and the splitting of 5d electrons of Eu^{2+} caused by changes in crystal field. The photoluminescence properties can be tailored by controlling the overall composition of the α-SiAlON host lattice.

References and Notes

(1) Krevel, J. W. H.; Hintzen, H. T.; Metselaar, R.; Meijerink, A. *J. Alloys Compd.* **1998**, *268*, 272.

(2) Uheda, K.; Endo, T.; Tamane, H.; Shimada, M.; Wang, C. M.; Mitomo, M. *J. Lumin.* **2000**, 87−89, 967.

(3) Hoppe, H. A.; Lutz, H.; Morys, P.; Schnick, W.; Seilmeier, A. *J. Phys. Chem. Solids* **2000**, *61*, 2001.

(4) Jansen, M.; Letschert, H. P. *Nature (London)* **2000**, *404*, 980.

(5) Krevel, J. W. H.; Rutten, J. W. T.; Mandal, H.; Hintzen, H. T.; Metselaar, R. *J. Solid State Chem.* **2002**, *165*, 19.

(6) Xie, R.-J.; Mitomo, M.; Uheda, K.; Xu, F.-F.; Akimune, Y. *J. Am. Ceram. Soc.* **2002**, *85*, 1229.

(7) Xie, R.-J.; Hirosaki, N.; Mitomo, M.; Yamamoto, Y.; Ohashi, N. *J. Am. Ceram. Soc.*, in press.

(8) Nakamura, S.; Fasol, G. *The Blue Laser Diode: GaN Based Light Emitters and Lasers*; Springer-Verlag: Berlin, 1997.

(9) Hampshire, S.; Park, H. K.; Thompson, D. P.; Jack, K. H. *Nature (London)* **1978**, *274*, 31.

(10) Ekstrom, T.; Nygren, M. *J. Am. Ceram. Soc.* **1992**, *75*, 259.

(11) Cao, G. Z.; Metselaar, R. *Chem. Mater.* **1991**, *3*, 242.

(12) Izumi, F.; Mitomo, M., Suzuki, J. *J. Mater. Sci. Lett.* **1982**, *1*, 533.

(13) Xie, R.-J.; Mitomo, M.; Xu, F.-F.; Uheda, K.; Bando, Y. *Z. Metallkd.* **2001**, *92*, 931.

(14) Blasse, G.; Grabmaier, B. C. *Luminescent Materials*; Springer-Verlag: Berlin, 1994.

(15) Butler, M. A. *J. Appl. Phys.* **1977**, *48*, 1914.

(16) Tang, J. W.; Zou, Z. G.; Ye, J. H. *J. Phys. Chem. B* **2003**, *107*, 14265.

(17) Ching, W.-Y.; Huang, M.-Z.; Mo, S.-D. *J. Am. Ceram. Soc.* **2000**, *83*, 780.

(18) Qiu, J.; Miura, K.; Sugimoto, N.; Hirao, K. *J. Non-Cryst. Solids* **1997**, *213−214*, 266.